Fuel, Volume 189, February 2017, pp. 98–106
DOI:10.1016/j.fuel.2016.10.080

Nitrogen and sulfur conversion during pressurized pyrolysis under CO_2 atmosphere in fluidized bed

Yuanqiang Duan [a], Lunbo Duan [a, b, *], Edward John Anthony [b], Changsui Zhao [a]

* Corresponding author: duanlunbo@seu.edu.cn

[a] Key Laboratory of Energy Thermal Conversion and Control, Ministry of Education, School of Energy and Environment, Southeast University, Nanjing 210096, China

[b] Centre for Combustion and CCS, Cranfield University, Cranfield, Bedfordshire MK43 0AL, UK

Abstract: Pressurized oxy-fuel combustion (POFC) is a promising technology for CO_2 capture from coal-fired power plants, offering both high efficiency and a low penalty. However, the high partial pressure of CO_2 in a POFC furnace has important impacts on fuel-N and fuel-S conversion during the coal pyrolysis process, and understanding this will help to achieve further control of SO_x/NO_x. In this study, coal pyrolysis experiments were conducted in a pressurized fluidized bed with the pressure range of 0.1-0.7MPa under N_2 and CO_2 atmosphere. The gaseous products were monitored by a Fourier transform infrared spectroscopy analyzer (FTIR) and the char residue was characterized by an X-ray photoelectron spectroscopy (XPS) analyzer in order to acquire the species information for S-containing and N-containing compounds. Results show that the enrichment of CO_2 in the local atmosphere enhances the fuel-N conversion to HCN in the pyrolysis process, which serves as a favorable precursor to N_2O. The generation of HCN and NH_3 increase simultaneously with the increase of overall pressure. SO_2 concentration in the gaseous product is relatively low, and as the pressure increases, the concentration decreases slightly due to CO reduction of SO_2 to COS. Sulfur content in the char decreases as the pressure goes from 0.1MPa to 0.7MPa indicating higher CO_2 pressure accelerates the decomposition of sulfur compounds in the coal, which is further confirmed by the XPS results.

Key words: pressurized oxy-fuel combustion; pyrolysis; CO_2 atmosphere; nitrogen conversion; sulfur speciation;

1. Introduction

Carbon capture and storage (CCS) technologies capture up to 90% of CO_2 emissions from a power plant or industrial facility and store them in underground geologic formations. The International Energy Agency (IEA) estimates that CCS can achieve 13% of the global greenhouse gas emissions reductions needed by 2050 to limit global warming to 2°C [1]. Carbon capture has been established for some industrial processes, but it is still a relatively expensive technology. Much effort needs to be devoted to reducing the cost of CCS technologies in the near future.

Oxy-fuel technology, as one of the major coal-fired power plant CCS technologies, has received much attention recently. In oxy-fuel technology, the process typically entails burning the fuel in a mixture of recycled flue gas and O_2 instead of air as the primary oxidant. The high CO_2 concentration in the flue gas makes it conducive to CO_2 separation. Also, other gaseous pollutants such as NO_x and SO_x can be simultaneously removed [2]. The biggest obstacle to the development and application of oxy-fuel technology at present is the net efficiency penalty associated with the high cost of the air separation unit (ASU) and compression purification unit (CPU). For a conventional air-fired coal power plant, the net efficiency reduced by more than 10% when it is converted to oxy-firing [3-5].

In the first generation oxy-fuel technology, the ASU and CPU run under pressure, while the boiler is run at atmospheric pressure. Thus, the pressure fluctuation associated with the ASU, boiler and CPU cause energy losses and a reduction of net efficiency. However, for second generation oxy-fuel technology, or pressurized oxy-fuel combustion (POFC) technology, the whole system runs under pressure, and hence the work losses due to the pressure fluctuations can be substantially reduced. Together with this feature, many other advantages can also be achieved by deploying POFC [6-8] including: (1) recovering latent heat from flue gas; (2) increasing the convective heat transfer for a given mean velocity; (3) reducing the boiler size and equipment costs; (4) avoiding air ingress, thus ensuring the production of high purity of CO_2 in the flue gas and a relatively low purification cost; and (5) reducing the cost of flue gas recirculation fan and

55 the CPU system.

56 To date, many studies have contributed to the optimization of the POFC systems. Hong et al.
57 [9,10] analyzed the ISOTHERM® pressurized oxy-combustion system of ENEL [11], and found
58 the maximum efficiency could be achieved in the vicinity of the 1.0MPa operating pressure. The
59 net efficiency showed nearly 3% increment at 1.0MPa over atmospheric combustion. Gopan et al.
60 [12,13] introduced a staged pressurized oxy-combustion (SPOC) system with fuel staging and low
61 flue gas recycle rate. The simulation of thermal system showed the optimal pressure was around
62 1.6MPa and the SPOC process increased the net efficiency up to 6% over conventional
63 atmospheric oxy-combustion.

64 However, on the other hand, there are few experimental studies on the POFC. The only
65 reported work includes coal combustion on the pressurized thermo-gravimetric analyzer (PTGA)
66 [14-16] and fluidized bed [3,17]. Wang et al. [14] conducted the coal combustion experiments on
67 the PTGA and the results indicated the effects of pressure on coal ignition mode. With the
68 increase of pressure, the heterogeneous ignition at atmospheric pressure converted to
69 homogeneous ignition at low and medium pressures, and then converted back to heterogeneous
70 ignition at high pressure. Lasek et al. [3,17] investigated the effect of pressure on pollutant
71 emissions, using a laboratory scale fluidized bed with continuous-feeding and found that NO,
72 N_2O, SO_2 emission were reduced under higher pressures during oxy-combustion.

73 As the first step of coal combustion, pyrolysis has great impact on the subsequent reactions.
74 The conversion of N and S in the pyrolysis stage has an important influence on NO_x/SO_x emission
75 and the operation safety of CPU system [18,19]. CO_2 is a reactant in the char gasification reaction,
76 as well as one of the final product of coal pyrolysis, so the existence of high partial pressures of
77 CO_2 affects the yield of volatile and N/S conversion significantly. Li et al. [20-25] conducted a
78 series of studies on the pyrolysis characteristics of the Victorian brown coal, mainly focused on
79 the generation of NO_x precursors with different operating parameters like atmosphere and reactor
80 types. The experiments show that CO_2 atmosphere surrounding coal/char particles can greatly
81 affect the formation of NH_3 and HCN through its influence on the availability of H-radicals

[24,25]. The CO_2 atmosphere tends to reduce the formation of NH_3 and HCN if the thermal cracking of char generates a significant amount of H-radicals. Many efforts have been made to investigate the effects of other operation parameters like fuel type, temperature and heating rate on the formation of NO_x precursor during coal pyrolysis under CO_2 atmosphere, and findings suggest that the CO_2-C gasification rate and the opening of -CN bond greatly affect the formation of NH_3 and HCN [26,27]. However, these studies are limited to atmospheric pressure and there are still few studies about the effects of pressure on N conversion during coal pyrolysis under pure CO_2 atmosphere.

Previous studies [28-30] have also revealed that the sulfur-containing gas and residual sulfur content in char during CO_2 pyrolysis is highly depends on the minerals and sulfur forms in raw coal. Experimental work shows the high CO_2 concentrations may promote the CO_2 reduction reaction of pyrite and generate more Fe_3O_4, CO and SO_2 [31]. The results of pyrolysis experiment of coal under N_2 and CO_2 atmosphere by Karaca [32] indicate that CO_2 atmosphere has more effects on the organic sulfur removal at high temperatures. Carbonate in coal can promote the decomposition of organic sulfur, and inhibit the decomposition of pyrite, while the silicate seems to promote the conversion from easily removable organic sulfur compounds to thermal stable organic sulfur compounds. At the same time, the effect of pressure on sulfur conversion during pyrolysis has mostly focused on pressurized hydro-pyrolysis studies, which showed that the increase of hydrogen pressure enhanced the removal of sulfur from coal [33,34].

Currently, information on N/S conversion of coal during pressurized pyrolysis under CO_2 atmosphere is still limited, and a more complete understanding of the pathway for fuel-N and fuel-S conversion is important for future work on POFC technology, and in particular for gaseous pollutant control and system optimization. This information will also help to build up a comprehensive model of the PFOC by providing detailed reaction mechanisms. In this study, experiments on a lab-scale pressurized fluidized-bed system have been done to help determine the influence of pressure on the N/S conversion into both gaseous and solid products.

2. Experimental

2.1 Fuel and bed material

Table 1 shows the ultimate and proximate analysis of the bituminous coal used in the experiment. The sulfur speciation in the raw coal was determined according to the Chinese standard method (GB/T 215-2003), and is shown in Table 2. The particle size of coal ranged from 0.45 to 0.60mm. Silica sand (particle size: 0.25 to 0.35mm, true density: 2600kg/m^3) was used as bed material, giving a static bed height of 0.3m.

2.2 Apparatus and procedure

Experiments were conducted on a 20kW$_{th}$ lab-scale pressurized fluidized bed system, as shown in Fig. 1, which consists of a bubbling fluidized bed combustor, gas distribution, feeding system, temperature and pressure controlling system, flue gas cooling system, and the gas analyzers. The combustor was made of the stainless steel, with an inner diameter of 50mm and a height of 1300mm. The combustor was placed in a pressure vessel, which was designed to withstand a pressure of 2.0MPa at 200°C. The bottom of the windbox was open, permitting the pressurized gas flowing into the riser to pass through it. During the experiments, the gas went into the pressure vessel first, and was heated by the reactor wall and then flowed into the windbox. However, because of this design, the pressure vessel is not operated at high temperature (<100°C). The flue gas leaving the reactor was then cooled down to 200°C by the gas cooler before entering the sampling line. A regulating valve was used at the outlet of the cooler to control the reaction pressure in the riser. The gas sampling line was connected to the sampling port after the regulating valve. The sampling line was electrically heated to control the temperature to around 165°C, to avoid the gas condensation. A filter was used to remove fine particles larger than 0.1μm from the flue gas. The Fourier transform infrared spectroscopy (FTIR) analyzer (Antaris IGS, Thermo Fisher Scientific Inc, USA) was used to monitor the composition of flue gas. The measuring accuracy of HCN/NH_3/SO_2 was 0.01ppm.

The coal pyrolysis characteristics under N_2 and CO_2 atmosphere were investigated with the operation pressure ranging from 0.1 to 0.7MPa. The bed temperature in the dense zone was

135 controlled at 750°C, 800°C, 850°C and 900°C, respectively. Batch feeding was used in this
136 experiment to avoid the unstable coal feeding under high pressure operation. Typically, 3-9g coal
137 particles with the desired size were injected into the bottom zone of the reactor by the pressurized
138 carrier gas. The gas velocity in the riser was normally in the range of 0.7-1m/s to guarantee the
139 good fluidization of the silica sand bed material. Each test run was repeated 3-5 times to minimize
140 the uncertainty in experiments.

141 *2.3 Analysis methods of char*

142 After each test, bed material was drained and char was removed by hand. This was easy to do
143 since the colour of the coal char and sand are very different. The char produced at 850°C and CO_2
144 atmosphere was collected and analysed by a CTS5000B sulfur analyzer in order to obtain the
145 sulfur content in the char. An X-ray photoelectron spectroscopy (XPS) analyzer (Escalab250Xi,
146 Thermo Scientific Inc) was used to quantify the S form at the char surface. The XPS
147 measurements in this study were carried out with an unmonochromated AlKα (1486.6eV)
148 radiation. The step size was set as 0.1eV, and the internal standard calibration was set as C1*s*
149 (284.6eV). The spectral features of S2*p* peak were used for sulfur speciation analysis.

150 In XPS analysis, the peak-fitting method is often chosen to identify the sulfur forms. The
151 reliability of the peak data is highly dependent on the specific method and parameter setting of
152 peak-fitting, and the two most common methods are $2p_{3/2}/2p_{1/2}$ doublet fitting and $2p_{3/2}$ single
153 peak fitting.

154 Based on previous studies [35-37] and the XPS database of American National Institute of
155 Standards and Technology (NIST) [38], the S2$p_{3/2}$ binding energies are summarized in Table 3.
156 Each sulfur specie in Table 3 refers to a class of chemicals except pyrite. The binding energy of
157 pyrite and sulfide have overlapping parts. Pyrite is the main sulfide components in coal, followed
158 by marcasite, sphalerite and galena. In this paper, S content in coal is divided into five categories:
159 sulfide/pyrite, thiophene, sulfoxide, sulfone and sulfate. The S2$p_{3/2}$ peak of sulfide is classified as
160 pyrite. The XPS peakfit 4.1 software was used in the peak analysis and parameters setting is
161 mainly based on the following principles [39]: (i) a 2:1 relative area was separated by 1.18 eV; (ii)

the L–G% (Lorentzian–Gaussian%) was set as 0; and (iii) the full width at half-maximum (FWHM) was set to the same value for each peak ranging from 0 to 2.

3. Results and Discussion

3.1 Fuel-nitrogen releasing during pyrolysis

Pyridines, pyrrole, and quaternary nitrogen are the three principal N-compounds in the coal. Previous study shows that part of the pyridines and pyrrole nitrogen are converted to HCN during pyrolysis process [40]. The formation of NH_3 has two main sources: one is the decomposition of quaternary nitrogen, while the other is the secondary reaction of tar and char. Fig. 2 presents the concentration of nitrogen-containing gases during coal pyrolysis under N_2 and CO_2 atmosphere at 0.5MPa and 850°C. NH_3 and HCN are the major nitrogen-containing gases during coal pyrolysis, while NO and N_2O can also be detected in the gases produced. Because of the very low concentration of NO and N_2O, their curves are not included in Fig. 2. The NH_3/HCN ratios under both atmospheres are relatively low in this study, a result which is very different with that previously reported [24]. This difference may be caused by the differences in quaternary nitrogen content in various coals. Also from Fig. 2, the HCN concentration in CO_2 atmosphere is higher than that in N_2 atmosphere, owing to strong C/CO_2 reaction in CO_2 atmosphere. The gasification process breaks the stable –CN bonds and make it much easier to form HCN.

The HCN release profiles in different temperature at 0.5MPa and CO_2 atmosphere are shown in Fig. 3. The peak value of HCN concentration curve increases as the pyrolysis temperature increases. As mentioned above, most of the HCN originates from the thermal-stable pyridines and pyrrole nitrogen in coal, and the higher temperature will increase their decomposition and generate more HCN [41]. In terms of nitrogen conversion, the nitrogen converted to HCN in CO_2 and N_2 atmosphere is 5.45 and 3.01 times of that converted into NH_3 in N_2 atmosphere. The existence of CO_2 during pyrolysis clearly enhances total nitrogen conversion rate of coal. In Fig. 3, the higher pyrolysis temperature leads to a shorter time for HCN concentration to reach its peak value. This also can be explained by the thermal-stability of pyridines and pyrrole nitrogen.

Fig. 4 and Fig. 5 show the N-containing gases release profiles of coal at different pressure

and atmospheres. For the NH_3 obtained in both atmospheres, with the increase of pressure the peak value of NH_3 concentration shows a slight increase. The quaternary nitrogen is completely decomposed over 800°C [40]. Therefore, the influence of the pressure on the quaternary nitrogen decomposition at 850°C should be negligible. In addition, the direct hydrogenation of char-N by H-radicals is another important source of NH_3 in the volatiles [22]. Higher pressure would slow down the diffusion of volatile precursors out from inside the particle, leading to increases in the residence time of volatile precursors inside the particles. This in turn intensify the thermal cracking of volatile precursors to produce more radicals, including H-radicals, and allow more time for the H-radical-laden volatile precursors to interact with the char-N to form NH_3.

From 0.1MPa to 0.7MPa the peak value of HCN concentration in N_2 and CO_2 atmosphere experienced a gradual rise. Pyridines and pyrrole nitrogen have a high thermal-stability, and are difficult to completely decompose even at 1000°C. However, high pressure is advantageous in enhancing the degree of pyrolysis, and the strong C/CO_2 reaction in pressurized CO_2 atmosphere breaks the stable -CN bonds of coal. And the exposed -CN sites encourage the formation of HCN with H-radical. It can be concluded that higher pressures enhance the generation of NO_x precursors.

Fig. 6 presents the conversion rate under different temperature and pressure. Raising the temperature at each operating pressure will lead an incense to fuel-N conversion rate. At 0.1MPa, the nitrogen conversion rate from 750°C to 900°C increased by 4.49%. While at 0.7MPa, this increase is about 12.78%. Thus it is clear that increasing temperature and pressure jointly promote the conversion of fuel-N to NO_x precursors.

3.2 Sulfur conversion during pressurized pyrolysis

H_2S and COS were not monitored in this study, however the sulfur content and sulfur speciation in the char residue were carefully investigated to provide us with additional information to better understand the sulfur chemistry under these conditions. During coal pyrolysis under CO_2 atmosphere, SO_2 concentration in the gaseous product was monitored and the curves of SO_2 under different pressure are shown in Fig. 7. SO_2 concentration in the gaseous product is relatively low,

however as the pressure increases, this concentration has a slight decrease. Another interesting result is that the elevation of pyrolysis pressure leads to a reduction in the amount of sulfur in the char. The sulfur content in the char residue at 850°C is shown in Table 4. As the pressure increases, the sulfur content in char decrease, indicating that more tar-S and volatile-S are generated. As SO_2 also decrease with pressure, there may be more COS or H_2S formation. By elevating the pyrolysis pressure, the high partial pressure of CO_2 enhances the formation of CO, which can be seen from Fig. 8. CO also appears to enhance the decomposition of sulfur in coal. This causes the drop of sulfur in char and creates more S-containing gases like H_2S and COS. The high concentration of CO also enhances the conversion reaction from SO_2 to COS [28], as R1and R2 show:

$$CO + SO_2 \rightarrow S + CO_2 \quad \text{R1}$$

$$CO + S \rightarrow COS \quad \text{R2}$$

However, this is only one possible route for the simultaneous reduction of SO_2 and char residue sulfur as the pressure increases, and more experiments with accurate measurement of H_2S and COS must be made to verify this explanation.

Fig. 9 shows the S2$p_{3/2}$ and S2$p_{1/2}$ doublet fitting results of raw coal and char obtained from pyrolysis under different pressures. In XPS peak fitting, the percentage of each peak area in relation to the total area is equated to the relative content of each sulfur form. Thus, based on the curve fitting results in Fig. 9, the distribution proportion of different sulfur forms is summarized in Table 5. The main sulfur forms in the raw coal surface is the sulfone (~37.32%) and thiophene (~23.29%), while the sulfide/FeS_2 only accounts for 16.04% of the total sulfur content of raw coal.

Sulfur conversion during coal pyrolysis is very complex. Sulfur-containing functional groups in coal decompose and release during pyrolysis process, and at the same time the interactions between pyrite, sulfate and organic sulfur also affect the distribution and speciation of sulfur in the final products. Zhang et al. [42] proposed a schematic of the sulfur conversion mechanisms during coal pyrolysis, as shown in Fig. 10, to illustrate the complex series of reactions.

For coal pyrolysis under high pressure CO_2 atmosphere, the reaction mechanism in Fig. 10

still applies. However, with different pressure, the rate and extent of each reaction will be different. Thus, for instance, the increase of pressure causes the pyrite content to generally decrease. In reductive atmosphere, the decomposition reaction of FeS_2 is mainly controlled by the following reaction:

$$FeS_2+CO \rightarrow FeS+COS \qquad R3$$

The R3 reaction is one of the main sources of COS during coal pyrolysis. This reaction is very slow at 800°C [28]. Given the pyrolysis temperature and short residence time of coal in the fluidized bed, part of FeS_2 will be converted to FeS, and will resist further reaction. The elevation of pressure enhances the reductive atmosphere through producing more CO, and accelerates the consumption rate of pyrite, so the pyrite content decreases when pressure increases.

The main kinds of sulfate in coal are the mixtures of $BaSO_4$, $CaSO_4 \cdot 2H_2O$, $CaSO_4$ and $FeSO_4$, and these sulfates in the raw coal are typically only present at about 0.31% as shown in Table 2. Fig. 9 and Table 5 show the change of sulfate content is not obvious under different pressure. Two facts can be deduced about the influence of pressure on sulfate. One is that as the pressure increases, the sulfur fixation ability of the coal ash is likely to be enhanced [43], given that calcium, potassium and sodium in the ash can capture the SO_2 in the gas more efficiently. The other is that as the pressure increase, higher concentration of CO will react with the sulfate to form SO_2, as show below:

$$MSO_4+CO \rightarrow MO+SO_2+CO_2 \qquad R4$$

Here M represents an alkali or alkaline earth metal. In addition, the reaction rate increases as the CO partial pressure increase. However, given that SO_2 levels were not shown to be high in this study, we believe the first explanation is likely to be the more important one, and indeed we can see the overall sulfate content under high pressure is higher than that in low pressure.

Thiophene, sulfoxide and sulfone are usually referred to as organic sulfur in coal. The composition and structure of organic sulfur are very complex and with the total different thermal stability. Thiophene is much more stable and difficult to decompose because sulfur in the thiophene is aromatically bound [28]. The thiophene in coal can be generated from the two

reactions as shown in Fig. 10, one is S or H_2S react with the organic matter in coal; The other is the pyrite reacts with small organic molecules like ethylene. When pyrolysis pressure increases, the relative content of thiophene will also rise. High pressure CO_2 promotes the gasification of coal and increases the concentration of small organic molecules, thus accelerating the generation of thiophene. Moreover, the decomposition of pyrite and sulfone reduces the total amount of sulfur in char under high pressure, so the relative content of thiophene which is thermal stable will increase.

Compared with the S2 curves, the specific components of S3 and S4 curves are much more complex and difficult to specify. The thermal stability of sulfoxide and sulfone is highly dependent on the functional groups contacted with -SO_2- and -SO-. Previous study [44] shows the thermal stability of sulfoxide and sulfone as follows: alphatic sulfoxide < aromatic sulfoxide < sulfone < 650°C. So sulfoxide and sulfone decompose at experimental condition (850°C). The pyrolysis of coal makes the conversion of sulfoxide and sulfone into gaseous products, and the removal rate of them increase with the increase of pressure and the degree of gasification.

In summary, the possible pathway of how the high pressure CO_2 atmosphere affects sulfur conversion during pyrolysis appear to be as follows: (1) high pressure increases the sulfur conversion rate, resulting in more gaseous products like COS; (2) high partial pressure of CO accelerates the decomposition of pyrite; (3) the sulfur fixation ability of the ash is further enhanced by high pressure; (4) high pressure increases the conversion from gaseous S and pyrite to thiophene.

4. Conclusion

Experiments on pyrolysis of coal at CO_2 atmospheres were conducted in a lab-scale pressurized fluidized bed system, and the influence of pressure on N and S conversion was explored. Some general conclusions can be drawn as follow:

1) For the raw coal in this experiment, HCN is the major nitrogen-containing gaseous product for coal pyrolysis at CO_2 atmosphere.

2) The generation of HCN and NH_3 increase simultaneously with the increase of overall pressure. High pressure and the existence of high partial pressures of CO_2 enhance the fuel-N conversion rate in pyrolysis process.

3) SO_2 concentration in gaseous product and sulfur content in char decrease simultaneously with the increase of overall pressure, indicating that more COS and H_2S are generated during the pyrolysis process.

4) The effects of high pressure CO_2 on the migration of sulfur during pyrolysis are mainly due to the changes of volatile yield and the rate of sulfur conversion reactions. High pressure of CO_2 accelerates the decomposition of pyrite and also intensifies the conversion from gaseous S and pyrite to thiophene.

Acknowledgements: This work was financially supported by the National Natural Science Foundation of China (No.51206023).

References

[1] Carbon Capture and Storage: The solution for deep emissions reductions, IEA, 2015.

[2] Chen L, Yong S Z, Ghoniem A F. Oxy-fuel combustion of pulverized coal: Characterization, fundamentals, stabilization and CFD modeling[J]. Progress in Energy and Combustion Science, 2012,38(2):156-214.

[3] Lasek J A, Janusz M, Zuwała J, et al. Oxy-fuel combustion of selected solid fuels under atmospheric and elevated pressures[J]. Energy, 2013,62:105-112.

[4] Escudero A I, Espatolero S, Romeo L M, et al. Minimization of CO_2 capture energy penalty in second generation oxy-fuel power plants[J]. Applied Thermal Engineering, 2016,103:274-281.

[5] Darde A, Prabhakar R, Tranier J, et al. Air separation and flue gas compression and purification units for oxy-coal combustion systems[J]. Energy Procedia, 2009,1(1):527-534.

[6] Xia F, Yang Z, Adeosun A, et al. Pressurized oxy-combustion with low flue gas recycle:

317 Computational fluid dynamic simulations of radiant boilers[J]. Fuel, 2016.

318 [7] Zebian H, Mitsos A. Pressurized OCC (oxy-coal combustion) process ideally flexible to the
319 thermal load[J]. Energy, 2014,73:416-429.

320 [8] Zebian H, Gazzino M, Mitsos A. Multi-variable optimization of pressurized oxy-coal
321 combustion[J]. Energy, 2012,38(1):37-57.

322 [9] Hong J, Chaudhry G, Brisson J G, et al. Analysis of oxy-fuel combustion power cycle
323 utilizing a pressurized coal combustor[J]. Energy, 2009, 34(9): 1332-1340.

324 [10] Hong J, Field R, Gazzino M, et al. Operating pressure dependence of the pressurized oxy-fuel
325 combustion power cycle[J]. Energy, 2010, 35(12): 5391-5399.

326 [11] Gazzino M, Benelli G. Pressurised oxy-coal combustion Rankine-cycle for future zero
327 emission power plants: process design and energy analysis[C]//ASME 2008 2nd International
328 Conference on Energy Sustainability collocated with the Heat Transfer, Fluids Engineering,
329 and 3rd Energy Nanotechnology Conferences. American Society of Mechanical Engineers,
330 2008: 269-278.

331 [12] Gopan A, Kumfer B M, Phillips J, et al. Process design and performance analysis of a Staged,
332 Pressurized Oxy-Combustion (SPOC) power plant for carbon capture[J]. Applied Energy,
333 2014, 125: 179-188.

334 [13] Gopan A, Kumfer B M, Axelbaum R L. Effect of operating pressure and fuel moisture on net
335 plant efficiency of a staged, pressurized oxy-combustion power plant[J]. International Journal
336 of Greenhouse Gas Control, 2015, 39: 390-396.

337 [14] Wang C, Lei M, Yan W, et al. Combustion characteristics and ash formation of pulverized
338 coal under pressurized oxy-fuel conditions[J]. Energy & Fuels, 2011, 25(10): 4333-4344.

339 [15] Lei M, Huang X, Wang C, et al. Investigation on SO_2, NO and NO_2 release characteristics of
340 Datong bituminous coal during pressurized oxy-fuel combustion [J]. Journal of Thermal
341 Analysis and Calorimetry, 2016. doi:10.1007/s10973-016-5652-y

[16] Ying Z, Zheng X, Cui G. Pressurized oxy-fuel combustion performance of pulverized coal for CO_2 capture[J]. Applied Thermal Engineering, 2016, 99: 411-418.

[17] Lasek J A, Głód K, Janusz M, et al. Pressurized oxy-fuel combustion: A Study of selected parameters[J]. Energy & Fuels, 2012, 26(11): 6492-6500.

[18] Pipitone G, Bolland O. Power generation with CO_2 capture: technology for CO_2 purification[J]. International journal of greenhouse gas control, 2009, 3(5): 528-534.

[19] Kim S, Ahn H, Choi S, et al. Impurity effects on the oxy-coal combustion power generation system[J]. International Journal of Greenhouse Gas Control, 2012, 11: 262-270.

[20] Xie Z, Feng J, Zhao W, et al. Formation of NO_x and SO_x precursors during the pyrolysis of coal and biomass. Part IV. Pyrolysis of a set of Australian and Chinese coals[J]. Fuel, 2001,80(15):2131-2138.

[21] Tan L L, Li C. Formation of NO_x and SO_x precursors during the pyrolysis of coal and biomass. Part II. Effects of experimental conditions on the yields of NO_x and SO_x precursors from the pyrolysis of a Victorian brown coal[J]. Fuel, 2000,79(15):1891-1897.

[22] Li C, Tan L L. Formation of NO_x and SO_x precursors during the pyrolysis of coal and biomass. Part III. Further discussion on the formation of HCN and NH_3 during pyrolysis[J]. Fuel, 2000,79(15):1899-1906.

[23] Tan L L, Li C. Formation of NO_x and SO_x precursors during the pyrolysis of coal and biomass. Part I. Effects of reactor configuration on the determined yields of HCN and NH_3 during pyrolysis[J]. Fuel, 2000,79(15):1883-1889.

[24] Jamil K, Hayashi J, Li C. Pyrolysis of a Victorian brown coal and gasification of nascent char in CO_2 atmosphere in a wire-mesh reactor[J]. Fuel, 2004,83(7-8):833-843.

[25] Chang L, Xie Z, Xie K, et al. Formation of NO_x precursors during the pyrolysis of coal and biomass. Part VI. Effects of gas atmosphere on the formation of NH_3 and HCN[J]. Fuel, 2003,82(10):1159-1166.

[26] Li X, Zhang S, Yang W, et al. Evolution of NO_x precursors during rapid pyrolysis of coals in CO_2 atmosphere[J]. Energy & Fuels, 2015,29(11):7474-7482.

[27] Duan L, Zhao C, Zhou W, et al. Investigation on coal pyrolysis in CO_2 atmosphere[J]. Energy & Fuels, 2009, 23(7): 3826-3830.

[28] Attar A. Chemistry, thermodynamics and kinetics of reactions of sulphur in coal-gas reactions: A review[J]. Fuel, 1978, 57(4): 201-212.

[29] Wang P, Jin L, Liu J, et al. Analysis of coal tar derived from pyrolysis at different atmospheres[J]. Fuel, 2013,104:14-21.

[30] Hu H, Zhou Q, Zhu S, et al. Product distribution and sulfur behavior in coal pyrolysis[J]. Fuel Processing Technology, 2004,85(8-10):849-861.

[31] Huang F, Zhang L, Yi B, et al. Transformation pathway of excluded mineral pyrite decomposition in CO_2 atmosphere[J]. Fuel Processing Technology, 2015,138:814-824.

[32] Karaca S. Desulfurization of a Turkish lignite at various gas atmospheres by pyrolysis. Effect of mineral matter[J]. Fuel, 2003,82(12):1509-1516.

[33] Chen H, Li B, Zhang B. Decomposition of pyrite and the interaction of pyrite with coal organic matrix in pyrolysis and hydropyrolysis[J]. Fuel, 2000, 79(13): 1627-1631.

[34] Xu W C, Kumagai M. Sulfur transformation during rapid hydropyrolysis of coal under high pressure by using a continuous free fall pyrolyzer[J]. Fuel, 2003, 82(3): 245-254.

[35] Grzybek T, Pietrzak R, Wachowska H. X-ray photoelectron spectroscopy study of oxidized coals with different sulphur content[J]. Fuel processing technology, 2002, 77: 1-7.

[36] Kozłowski M. XPS study of reductively and non-reductively modified coals[J]. Fuel, 2004, 83(3): 259-265.

[37] Marinov S P, Tyuliev G, Stefanova M, et al. Low rank coals sulphur functionality study by AP-TPR/TPO coupled with MS and potentiometric detection and by XPS[J]. Fuel processing technology, 2004, 85(4): 267-277.

[38] http://srdata.nist.gov/xps/selEnergyType.aspx

[39] Wang Z, Li Q, Lin Z, et al. Transformation of nitrogen and sulphur impurities during hydrothermal upgrading of low quality coals[J]. Fuel, 2016,164:254-261.

[40] Duan L, Zhao C, Ren Q, et al. NO_x precursors evolution during coal heating process in CO_2 atmosphere[J]. Fuel, 2011,90(4):1668-1673.

[41] Glarborg P. Fuel nitrogen conversion in solid fuel fired systems[J]. Progress in Energy and Combustion Science, 2003,29(2):89-113.

[42] Zhang D, Yani S. Sulphur transformation during pyrolysis of an Australian lignite[J]. Proceedings of the Combustion Institute, 2011, 33(2): 1747-1753.

[43] Zakkay V, Clisset H, Ganesh A, et al. Sulfur retention of North Dakota (Beulah) lignite ash in PFBC[C]//ASME 1984 International Gas Turbine Conference and Exhibit. American Society of Mechanical Engineers, 1984: V003T05A014-V003T05A014.

[44] Van Aelst J, Yperman J, Franco D V, et al. Study of silica-immobilized sulfur model compounds as calibrants for the AP-TPR study of oxidized coal samples[J]. Energy & fuels, 2000, 14(5): 1002-1008.

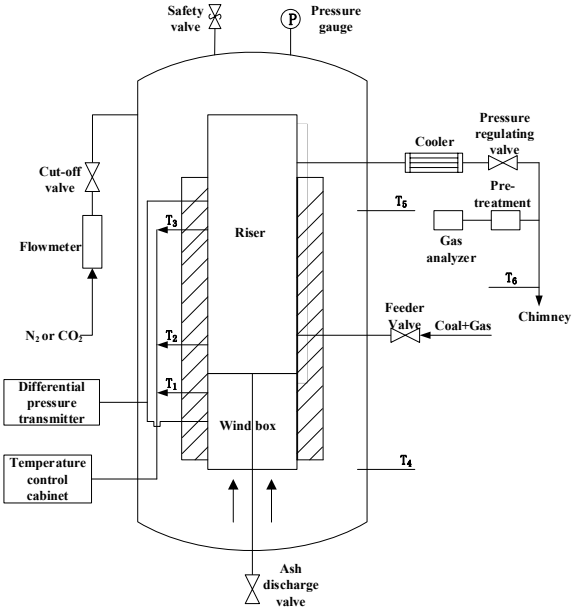

Fig. 1. Schematic diagram of pressurized fluidized bed system

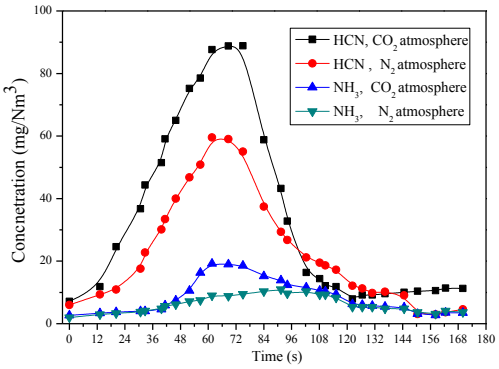

Fig. 2. Concentration of N-containing gases during coal pyrolysis at 0.5MPa and 850°C

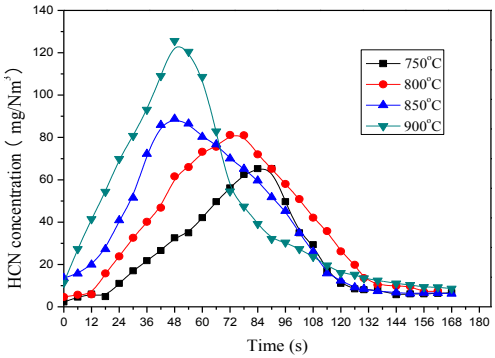

Fig. 3. HCN concentration curves of coal pyrolysis at 0.5MPa and CO_2 atmosphere

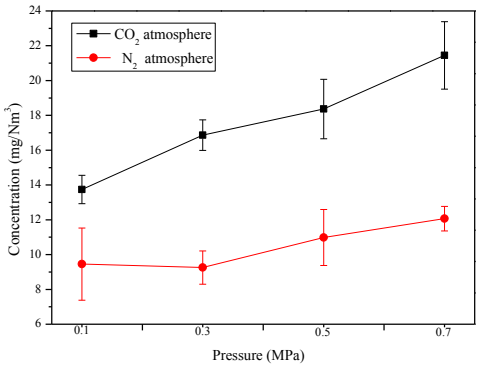

Fig. 4. NH_3 peak concentration at 850°C with different pressure

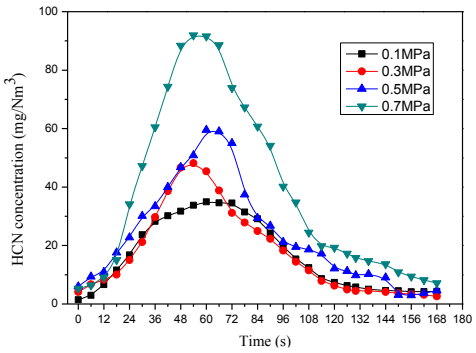

(a) N_2 atmosphere

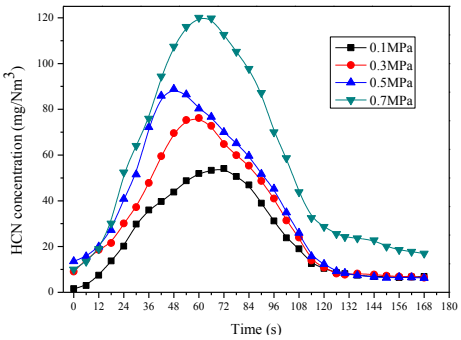

(b) CO_2 atmosphere

Fig. 5. HCN release curves of coal pyrolysis at 850°C with different pressure

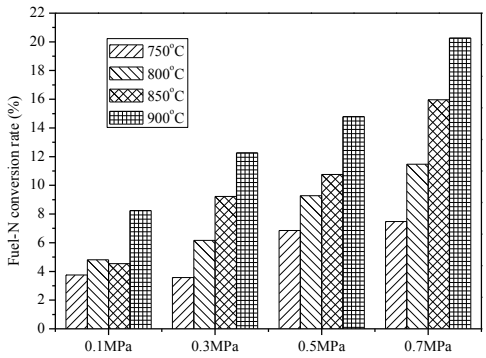

Fig. 6. Fuel-N conversion rate under CO_2 atmosphere at different temperature and pressure

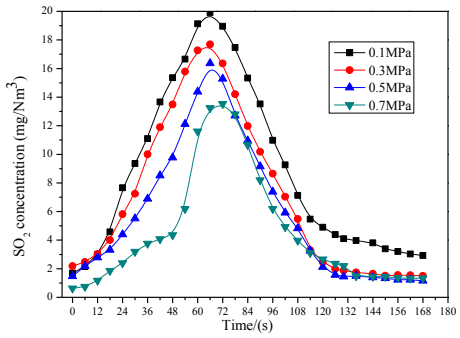

Fig. 7. SO_2 release curves of coal pyrolysis at 850°C and CO_2 atmosphere with different pressure

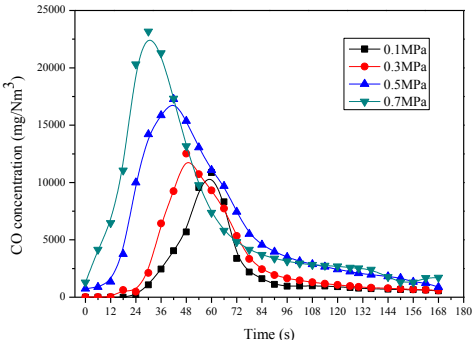

Fig. 8. CO release curves of coal pyrolysis at 850°C and CO_2 atmosphere with different pressure

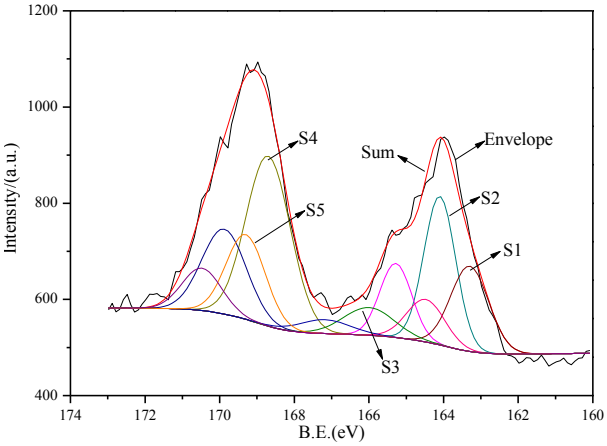

(a). Raw coal

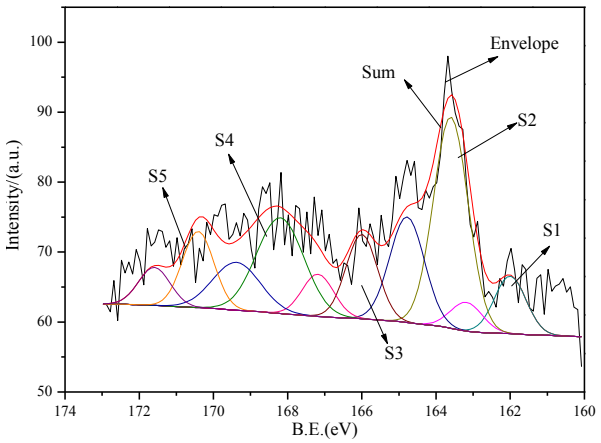

(b). Char under 0.1MPa

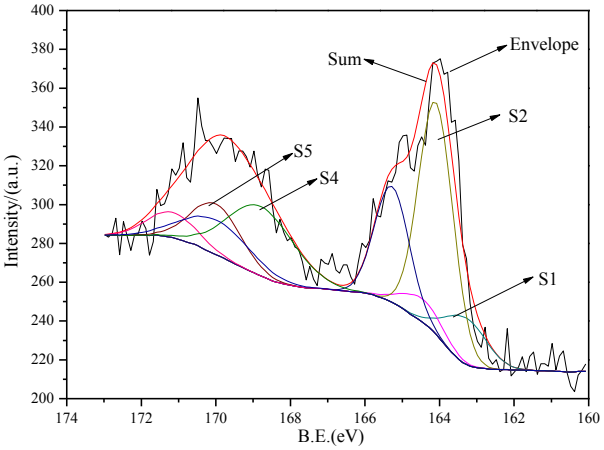

(c). Char under 0.3MPa

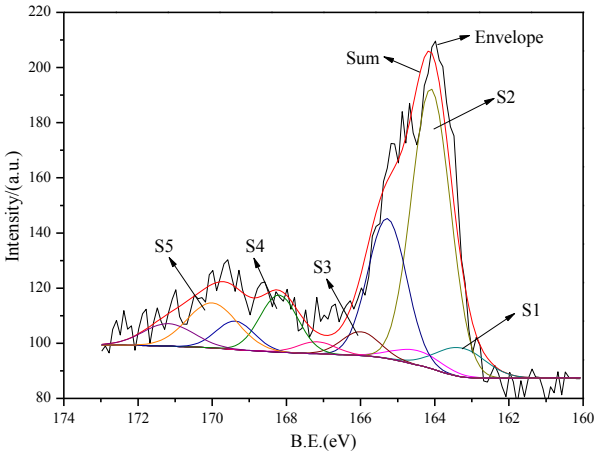

(d). Char under 0.5MPa

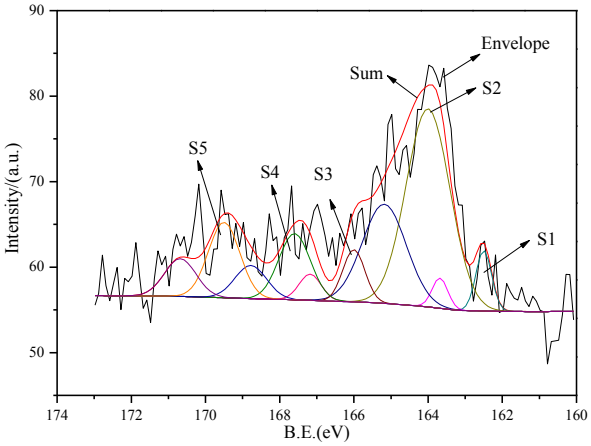

(e). Char under 0.7MPa

Fig. 9. Curve fitting results of raw coal and char

(S1-Pyrite peak; S2-Thiophene peak; S3-Sulfoxide peak; S4-Sulfone peak; S5-Sulfate peak)

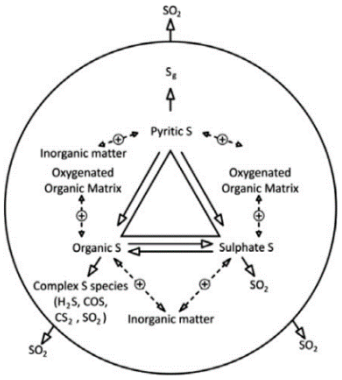

Fig. 10. A schematic of the mechanisms of sulfur conversion during coal pyrolysis [42]

Table 1. Ultimate and proximate analysis of raw coal / %

Coal	Ultimate analysis						Proximate analysis			Lower calorific value/
samples	$w(C_{ad})$	$w\ (H_{ad})$	$w\ (O_{ad})$	$w\ (N_{ad})$	$w\ (S_{ad})$	$w\ (M_{ad})$	$w\ (A_{ad})$	$w\ (V_{ad})$	$w\ (FC_{ad})$	($MJ•kg^{-1}$)
Raw coal	67.42	4.14	8.31	1.04	2.72	6.52	9.85	35.34	48.29	26.66

*ad denotes air dried basis

Table 2. Forms of sulfur in raw coal / %

Total sulfur	Pyrite sulfur	Sulfate sulfur	Organic sulfur
2.72	0.51	0.31	1.90

Table 3. Binding energies of S2$p_{3/2}$

Sulfur species	Binding energy (eV)
Pyrite	162.3-162.9
Sulfide	162.1-163.6
Thiophene	164.0-164.4
Sulfoxide	165.0-166.0
Sulfone	167.0-168.3
Sulfate	＞168.4

Table 4. Sulfur content in char under various pressures

Pressure/MPa	0.1	0.3	0.5	0.7
w(Sulfur content)/%	2.37	1.93	1.75	1.64

Table 5. Distribution proportion of different sulfur forms after the curve fitting procedure

Sulfur species	Sulfur content *w*/%				
	Raw coal	Char under 0.1MPa	Char under 0.3MPa	Char under 0.5MPa	Char under 0.7MPa
Sulfide/Pyrite	16.04	12.20	11.14	8.07	6.36
Thiophene	23.29	38.13	46.98	62.26	58.10
Sulfoxide	6.93	9.68	0.00	5.18	8.11
Sulfone	37.32	28.17	27.25	11.46	11.55
Sulfate	16.42	11.82	14.63	13.03	15.88